ELSEVIER

Magnetic Resonance Materials in Physics, Biology and Medicine 12 (2001) 104–113

MAGMA

Magnetic Resonance Materials in Physics, Biology and Medicine

www.elsevier.com/locate/magma

Specific targeting of folate–dendrimer MRI contrast agents to the high affinity folate receptor expressed in ovarian tumor xenografts

Sheela D. Konda [a,b,c], Michael Aref [a,b,d], Steven Wang [b,d], Martin Brechbiel [e], Erik C. Wiener [a,b,c,d,*]

[a] *Biomedical Magnetic Resonance Laboratory, College of Medicine, University of Illinois, Urbana, IL, USA*
[b] *The Beckman Institute, University of Illinois, Urbana, IL, USA*
[c] *Department of Molecular and Integrative Physiology, University of Illinois, Urbana, IL, USA*
[d] *Department of Nuclear, Plasma, and Radiological Engineering, University of Illinois, Urbana, IL, USA*
[e] *National Cancer Institute, National Institutes of Health, Bethesda, MD, USA*

Received 9 January 2001; accepted 11 January 2001

Abstract

The need to develop target-specific MRI contrast agents to aid in disease characterization remains highly essential. In this study, we present a generation four polyamidoamine (PAMAM) folate–dendrimer that specifically targets the high affinity folate receptor (hFR) overexpressed on more than 80% of ovarian tumors. In vitro, mouse erythroleukemia cells expressing the hFR bind the radiolabeled folate–dendrimer chelate resulting in over 2700% increase in binding compared with untreated cells. The binding was inhibited by free folic acid to levels observed on folate-receptor-negative cells. In vivo, ovarian tumor xenografts resulted in a 33% contrast enhancement, following the folate–dendrimer chelate administration, that was significantly different compared with results obtained with a non-specific, extracellular fluid space agent, Gd-HP-DO3A. In addition, this contrast enhancement was absent in saline-treated animals, folate-receptor-negative tumors, and was inhibited by free folic acid. Results suggest that a macromolecular, dendrimeric MRI agent with high molecular relaxivities (1646 mM^{-1} s^{-1}) can be used in specifically targeting the hFR on tumor cells and ovarian tumors.

Keywords: Folate; Dendrimer; Ovarian cancer; Targeted contrast agents; MRI; Gadolinium

1. Introduction

Ovarian cancer has the highest mortality rate of all gynecological malignancies in the US [1]. Many patients with epithelial ovarian cancer are often diagnosed following metastasis throughout the peritoneal cavity. Recently, imaging of ovarian cancer using a non-specific gadolinium agent was shown to provide additional clinically relevant information concerning residual or recurrent tumors that express normal CA-125 levels, a tumor-associated glycoprotein antigen that is monitored in the patient's serum lacking high specificity and sensitivity for ovarian cancer [2]. In addition, this contrast-enhanced imaging of ovarian cancer had superior sensitivity and accuracy in assessing disease status than CA-125 alone, but required an improvement in specificity. Low et al. also states the need for more sensitive and accurate tumor markers as well as imaging studies [2]. In this study, we present a folate-receptor targeted, macromolecular dendrimeric agent that should address the need for specificity in ovarian cancer diagnosis. In general, site-directed MR contrast agents should expand the diagnostic ability and use of MRI.

Macromolecular contrast agents (> 20000 Da) due to their larger size enable longer imaging times and possess higher relaxation rates resulting from their longer rotational correlation times [3,4]. These agents have been used to enhance tumors via active targeting. Active targeting utilizes a specific cell surface molecule that is either unique or overexpressed on the tissue of interest. This type of targeting is more challenging due

* Corresponding author. Present address: 1710 Beckman Institute, 405 North Mathews, Urbana, IL 61801, USA. Tel.: +1-217-2447193; fax: +1-217-2441330.
E-mail address: e-wiener@uiuc.edu (E.C. Wiener).

1352-8661/01/$ - see front matter
PII: S1352-8661(01)00106-5

to large amounts of magnetic label in the tissue of interest required in order to achieve a sufficient diagnostic signal. Unger et al. used an anti-carcinoembryonic antigen (CEA) antibody conjugated to ~1.5 Gd atoms/antibody to enhance human colon carcinoma implanted in the thighs of hamsters [5]. The accumulation of the anti-CEA antibody–Gd–DTPA conjugate in the tumor was too low to produce enhancement and suggests a need for agents to deliver larger amounts of gadolinium than can be directly attached to the antibody. To increase the number of gadolinium per antibody, polymeric gadolinium complexes were utilized where the ε-amino groups of poly-L-lysine were conjugated to approximately 65 Gd–DTPA molecules and then to an antibody with high specificity for colon carcinomas [6]. Though enough of the targeted agent accumulated in the tumor to result in signal enhancement, the large amount of protein necessary caused concerns with high production costs and future immunologic responses.

Particulate contrast agents based on magnetite, monocrystalline iron oxide nanoparticles (MION) and ultrasmall superparamagnetic particles of iron oxide (USPIO) have been selectively targeted to various organ systems and pathologies [7–14]. In addition to MIONs and USPIOs, active targeting has been achieved with antibody-conjugated paramagnetic liposomes (ACPL). Paramagnetic polymerized liposomes conjugated to an $\alpha_v\beta_3$ integrin-specific antibody has been targeted to tumor vasculature [15]. More recently, antibodies to the intercellular adhesion molecule-1 (ICAM-1) attached to ACPLs were targeted to microvasculature in mice with experimental autoimmune encephalitis [16].

Another way to amplify the amount of gadolinium reaching the tumor site is through the use of dendrimers as MRI contrast agents [17]. Dendrimer agents are very flexible agents with respect to their symmetry, size, and uniform surface chemistry allowing the conjugation of various targeting molecules of interest. In the ammonia core polyamidoamine (PAMAM) dendrimers, the first three arms conjugated to the central ammonia represent the zeroth generation (Fig. 1). As the generation number increases from 0 to 6, the number of peripheral groups follows the geometric series 3, 6, 12, 24, 48, 96, and 192.

Dendrimers were attached to target-specific moieties with active tumor targeting applications. Dendrimers were initially coupled with porphyrin, chelating radiocopper ions, and then to rabbit IgG [18]. These conjugates retained 90% of the immunoreactivity of the unmodified antibody and have potential applications in radioisotope targeting. Generation four PAMAM dendrimers have been used to increase the efficacy of boron neutron capture therapy by specifically targeting tumors [19]. Yang et al. shows that dendrimers conjugated to boronated epidermal growth factor were able to accumulate specifically in only epidermal growth factor receptor expressing high-grade gliomas in rats [19].

To address the need for target-specific MRI contrast agents with high relaxivity, we present dendrimers conjugated to folic acid and Gd–DTPA that can be used as efficient tumor-specific MRI contrast agents (Fig. 1). Previously, we have shown that cells expressing the folate receptor resulted in a specific increase of over 100% in longitudinal relaxation rate at 1T compared with untreated cells and that this increase is inhibited by folic acid [20]. When administered in vivo, the folate–dendrimer was shown to accumulate in xenografted ovarian tumors expressing the folate receptor resulting in a greater signal enhancement compared with a non-specific extracellular agent, Gd-HP-DO3A [21].

The use of antibodies as target-specific molecules experience problems that include rapid clearance by the reticuloendothelial system, decreased affinity of the antibody following conjugation of the magnetic label, circulating free antigen, insufficient tumor penetration, binding of antibodies to non-specific Fc receptors, and possible changes in the antigen over time [5,6,22]. To avoid these problems, targeting endogenous transport mechanisms within cells have been suggested, one of which is the recycling high affinity folate receptor (hFR) pathway [23–25]. Folic acid is an essential water-soluble vitamin that is utilized by mammalian cells during the biosynthesis of methionine, serine, deoxythymidylic acid, and purines.

Previous studies have shown that the expression of hFR is elevated in many tumors of epithelial origin compared with normal tissue [26,27]. Some of these epithelial tumors include: ovarian [26,28–34], lung [26,34], kidney [26,34], breast [26], colon [26,34], choriocarcinomas [26], childhood ependymomas [35], and choroid plexus brain tumors [26,34]. These studies have reported in detail the differential expression of the folate receptor in diseased tissue.

In this study, we tested the hypothesis that specific targeting of folate–dendrimer chelates can be shown in mouse erythroleukemia cells and in ovarian tumor xenografts expressing the hFR. Our in vitro results show that the folate–dendrimers labeled with ^{153}Gd specifically bind to folate-receptor-positive cells, this binding is significantly higher than in folate-receptor-negative cells, and inhibited by free folic acid. We also show that ovarian xenograft accumulation of the folate–dendrimer with MRI is specific and significantly different from saline, receptor-negative tumors, and following a simultaneous injection of free folic acid with the folate–dendrimer.

2. Materials and methods

2.1. Contrast agent

Fourth generation ammonia core PAMAM dendrimers were prepared as described by Wiener et al. [17]. The folate-conjugated dendrimer-chelate was prepared by coupling folate to the PAMAM via a carbodiimide reaction, followed by reacting the remaining free amines with 2-(4-isothiocyanatobenzyl)-6-methyl-diethylenetriamine pentaacetic acid [20]. Gadolinium was then complexed to the dendrimer-chelate by transmetalation in a citrate buffer, followed by extensive ultrafiltration. To produce the radioactive folate–dendrimer chelate used in the in vitro studies, radioactive ^{153}Gd was exchanged with the non-radioactive Gd for 1 week and followed by extensive filtration. Briefly, ultrafiltration membranes, Model YM1 and XM 50, 25 mm, were prepared according to manufacturer's instructions (Diaflo, Beverly, MA). Then, 1 ml of ~72.5 μM PAMAM folate–dendrimer, generation four, was added to 10 ml citric buffer, pH 6, to which 50 μCi of $^{153}GdCl_3$ tracer solution was added. This solution was incubated for 1 week, washed three times with 0.1 M acetate buffer at pH 6.4, followed by three washes with 0.1M EDTA, and three times with deionized water in the

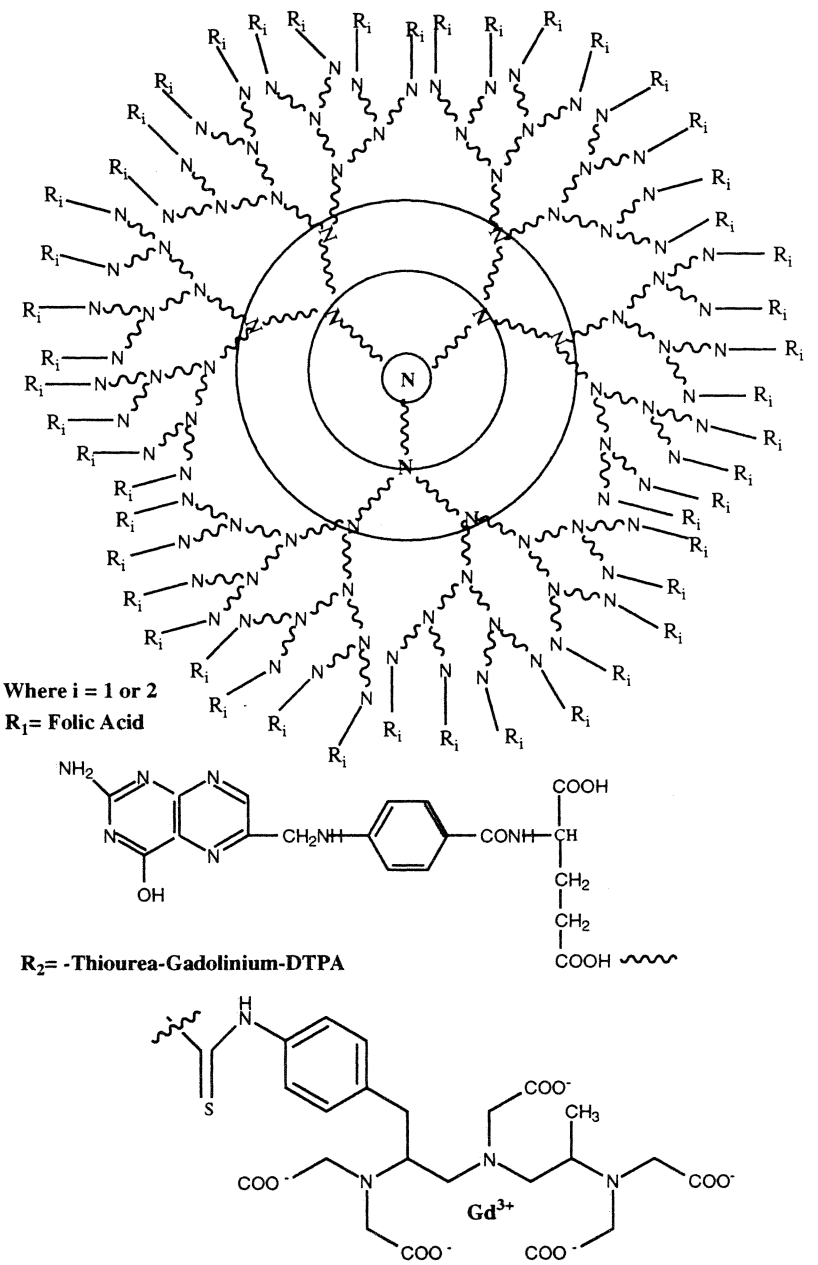

Fig. 1. A schematic of PAMAM generation four folate–dendrimer with 48 available conjugation sites. Of these, approximately 3–5 folic acids are conjugated to the dendrimer and the remaining contain gadolinium chelated with DTPA.

ultrafiltration cell at 55 psi argon. Gd-HP-DO3A (ProHance) was purchased from Bracco Diagnostics, Inc. (Princeton, NJ).

2.2. Tissue culture

Mouse erythroleukemia cells (MEL/FR −), a nM folate-receptor-negative cell line, and F2-MTX^{r}A/FR+ cells, a nM folate-receptor-positive cell line, were provided by Dr Edward Roy and Dr David Kranz from the University of Illinois, Urbana/Champaign.

The FR− cells were maintained in RPMI 1640 culture medium supplemented with 10% FBS, 2 mM L-glutamine, penicillin (100 U ml^{-1}), and streptomycin (100 μg ml^{-1}) (Sigma, St. Louis, MO). The FR+ cells were grown in the same conditions except that RPMI 1640 was replaced with folate-free RPMI 1640 (Life Technologies, Rockville, MD).

2.3. Animal model

Ovarian tumors were induced in female athymic *nu/nu* nude mice 5–6 weeks of age (Harlan Sprague Dawley, Inc. Indianapolis, IN) by subcutaneously injecting, ~ 10^{7}–10^{8}, human ovarian tumor cells expressing the hFR, OVCA 432 (provided by Dr R. Knapp, Dana Farber Institute, Boston, MA) or lacking the hFR, SKOV3 (ATCC # 7-HTB, Rockville, MD), in the subscapular area on the dorsal surface. Mice were housed in polycarbonate microisolator cages and tumor sizes were monitored three times per week. Tumors reaching a diameter of ~ 1 cm after 12–14 weeks (hFR-positive) or ~ 20 weeks (hFR-negative) of inoculation were used for MR experiments. One week prior to imaging, all animals were transferred from their normal rodent diet (Teklad, Indianapolis, IN) to one consisting of a folate-free rodent diet (Purina, Frankfort, IN).

2.4. In vitro specificity studies

The RPMI 1640 media from the receptor-negative mouse erythroleukemia cell line (MEL/FR −) was changed to folate-free 1640 media ~ 12 h prior to each experiment. This allowed the removal of bound folic acid from the minimally expressed receptors on these cells. The receptor-positive and receptor-negative cell lines were washed with 0.1% Dulbecco's phosphate-buffered saline (without Ca^{2+} and Mg^{2+})/bovine serum albumin (Sigma, St. Louis, MO) by centrifuging at 266 × *g* for 6 min. Cells were then aliquoted into microfuge tubes consisting of ~ 10^{7} cells ml^{-1}. Following a 10 min equilibriation at 37°C, the radioactive 1.64 μM ^{153}Gd–Folate–dendrimer (100 μl) was added to the receptor-positive and receptor-negative cells. For the competitive inhibition studies, free folic acid (0.8 μl of 17.8 mM) was added 15 min prior to the folate–dendrimer to the receptor-positive cells and all conditions were incubated for an additional 30 min at 37°C. Following the treatment, cells were washed twice with 0.1% Dulbecco's phosphate buffered saline (with Ca^{2+} and Mg^{2+})/bovine serum albumin by microfuging for 30 s. The cells were resuspended in 1 ml of 0.1% Dulbecco's phosphate buffered saline (without Ca^{2+} and Mg^{2+})/bovine serum albumin. Radioactivity was measured using the self-assembled Geiger–Müller (GM) counting system with a lead chamber (EG&G ORTECK, Oak Ridge, TN). All the samples were placed at the same geometry to minimize counting error. Background counts were subtracted from the counts of radioactive samples and normalized to 1 × 10^{6} cells.

2.5. Magnetic resonance imaging

Imaging experiments were performed on a Spectroscopy Imaging System Corporation (Fremont, CA) 4.7 *T*/33-cm bore system using a home-built 6-cm-diameter birdcage RF coil with a built-in gas mask [36] for delivery of 0.75–1% halothane/air mixture. A 27-gauge catheter (Baxter Healthcare Corporation, Deerfield, IL) was filled with ~ 100 μl heparinized saline (Abbott Laboratories, North Chicago, IL), followed by 10 μl air to prevent mixing, and 200 μl folate-conjugated dendrimer (0.056 mmol Gd kg^{-1}; $n = 5$ hFR-negative and hFR-positive tumors). For the free folate competition experiments ($n = 4$ of hFR-positive tumors with 0.3 mmol folic acid kg^{-1}), a simultaneous injection of the folic acid and the folate–dendrimer in 200 μl of HEPES buffer (Sigma, St. Louis, MO), pH = 7.4, was administered. Vehicle controls ($n = 5$ hFR-positive tumors) using 200 μl heparinized saline were also performed. Folate–dendrimer accumulation was compared with 200 μl of the non-specific agent, Gd-HP-DO3A (0.3 mmol Gd kg^{-1}; $n =$ 4 hFR-positive tumors). The catheter was inserted into the tail vein prior to placement of the animal in the magnet. A vial of 1 mM Gd-HP-DO3A was placed next to the animal and used to normalize signal intensity. A Deltaphase isothermal heating pad (Braintree Scientific, Inc., Braintree, MA) was placed over the RF coil to maintain body temperature.

A multi-slice (5) spin-echo imaging sequence was used to obtain sagittal (512 × 256) or transverse (256 × 256) slices under T_1-weighted (TR/TE 0.4/0.0169 s, ~ 15-min acquisition time) and T_2-weighted (TR/TE 4.0/0.04 s, ~ 30-min acquisition time) conditions. Images were acquired before contrast administration, immediately after contrast administration, and 24 h after contrast administration. The field of view was 12 cm × 6 cm or 6 cm × 6 cm for the sagittal images and transverse images, respectively.

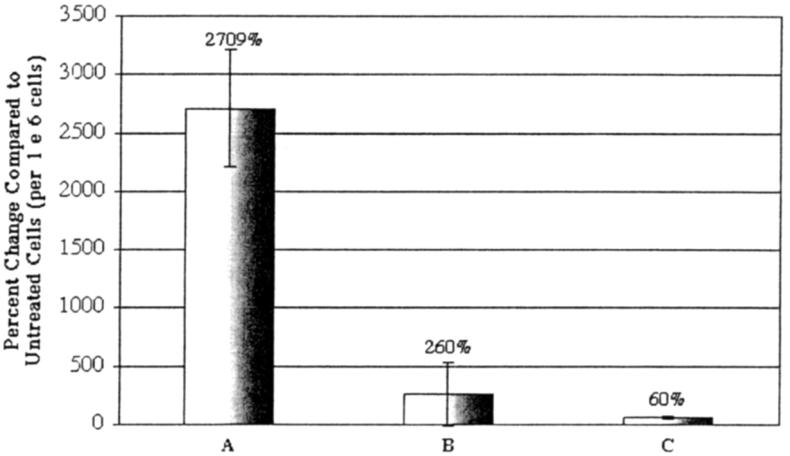

Fig. 2. In vitro binding of the radiolabeled ^{153}Gd–folate–dendrimer chelate occurs in folate-receptor-positive cells ($n = 6$), which is inhibited by free folic acid ($n = 6$), and does not bind to folate-receptor-negative cells ($n = 6$). In A, folate-receptor-positive cells were treated with 1.64 μM folate–dendrimer for 30 min at 37°C. In B, folic acid competition results are presented where folate-receptor-positive cells were pre-incubated with ~ 23-fold molar excess of free folic acid for 15 min followed by the folate–dendrimer for 30 min at 37°C. In C, folate-receptor-negative cells were treated with 1.64 μM folate–dendrimer. There is a significant increase in A compared with B and C ($P < 0.001$). The conditions B and C do not differ from each other ($P = 0.10$).

2.6. Image analysis

The T_1-weighted images were used to define the location of the tumor and to serve as an indicator of whether the tail vein injections were successful. Of the five slices obtained for each tumor, the top and bottom slices were not included in the data analysis to prevent confounding partial volume effects at the edges of the tumor.

The signal intensities within the region of interest (i.e. tumor or reference) were obtained using NIH image 1.61/ppc (NIH, Bethesda, MD). Tumor signal intensity was normalized to the 1 mM Gd-HP-DO3A reference to obtain a relative intensity (RI) at each of the imaging conditions (pre-injection, post-injection, or 24 h post-injection): RI = signal intensity of tumor divided by signal intensity of reference.

The percentage of contrast enhancement (PCE) was calculated according to the following

$$\mathrm{PCE} = \frac{\mathrm{RI_{post}} - \mathrm{RI_{pre}}}{\mathrm{RI_{pre}} \times 100\%}$$

$\mathrm{RI_{post}}$ was replaced with $\mathrm{RI_{post\ 24}}$ to obtain PCE after 24 h. All results were tested for significance using analysis of variance and the Wilcoxon rank-sum test.

3. Results

3.1. In vitro specificity studies

Prior to showing specificity of the folate–dendrimer binding in vivo with MRI, radioactive gadolinium-153, chelated to the folate–dendrimer was administered to mouse erythroleukemia cells in vitro. First, we wanted to test whether the folate–dendrimer chelate was able to bind to these cells which express the folate receptor. Results presented in Fig. 2 show that folate-receptor-positive cells administered with the 1.64 μM folate–dendrimer show $2709 \pm 540\%$ increase in binding compared with untreated cells. To determine if this binding was specific, a series of controls were performed. First, mouse erythroleukemia cells lacking the folate receptor were treated with the folate–dendrimer. There was a $59 \pm 11\%$ increase in binding compared with untreated cells. Second, cells expressing the folate receptor were first treated with free folic acid, followed by the folate–dendrimer. In this competition experiment, there was a $260 \pm 273\%$ increase in binding compared with untreated cells. The receptor-positive cells exhibited a significant increase in binding compared with both of the controls ($P < 0.001$). In addition, the receptor-negative control and the free folic acid competition binding results were not significantly different from each other ($P = 0.10$). These results suggest that not only was the folate–dendrimer able to bind to the cells, but the binding required the expression of the high affinity folate receptor and that the binding occurs via a saturable site that interacts with free folic acid.

3.2. In vivo specificity studies

Following the demonstration of the specificity of binding of the folate–dendrimer chelate in vitro, we next wanted to show that targeting of the folate–dendrimer to ovarian tumor xenografts generated in vivo with MRI. Previously, we have shown that the folate–dendrimer is able to accumulate in ovarian tumor xeno-

grafts expressing the hFR resulting in greater enhancement of the tumors compared with a non-specific agent, Gd-HP-DO3A in the same tumor type [21]. Following 24 h of injection, ovarian tumors expressing the hFR ($n = 5$) resulted in a 33.1% change in PCE under T_2-weighted conditions (Fig. 3). This was attributed to the high transverse relaxivity ($r_2 = 41.16 \pm 3.14$ mM^{-1} s^{-1}) of the folate–dendrimer at $4.7T$ compared with Gd-HP-DO3A ($r_2 = 4.89 \pm 0.16$ mM^{-1} s^{-1}). The change in PCE was greater compared with the non-specific agent post-injection, $n = 4$, ($P = 0.025$) and was significantly different from the non-specific agent 24 h post-injection ($P = 0.025$), Fig. 4. The latter result was expected since extracellular, fluid-space agents are usually not present 24 h following the injection due to their short half-life of 20 min in rats and 90 min in humans [3].

In this study, we tested the specificity of the folate–dendrimer binding to the hFR. Results calculating the PCE of the images following the injection and 24 h of the injection with the appropriate agent and tumor model are presented in Table 1. To determine whether the PCE observed in hFR-positive xenografts following the folate–dendrimer administration was due to the accumulation of gadolinium within the tumor and not some random partial volume effect associated with repositioning the animals in the machine 24 h later, a saline-treated animal was used as a control. Contrast enhancement following 24 h of a saline vehicle injection ($n = 5$) are significantly different from ovarian tumors expressing the hFR treated with the folate–dendrimer at the same time point, $P = 0.047$. In addition, the post-24 PCE of the folate–dendrimer is significantly different than the post-PCE observed with saline, $P = 0.011$. This provided additional evidence that the contrast enhancement originally observed is most likely due to the presence of the folate–dendrimer and not from misalignment of the tumor slices.

Next, we wanted to see if the accumulation requires the expression of the hFR. T_2-weighted images of ovarian tumor xenografts prepared with cells that lack hFR, SKOV3 ($n = 5$), showed no significant decrease in

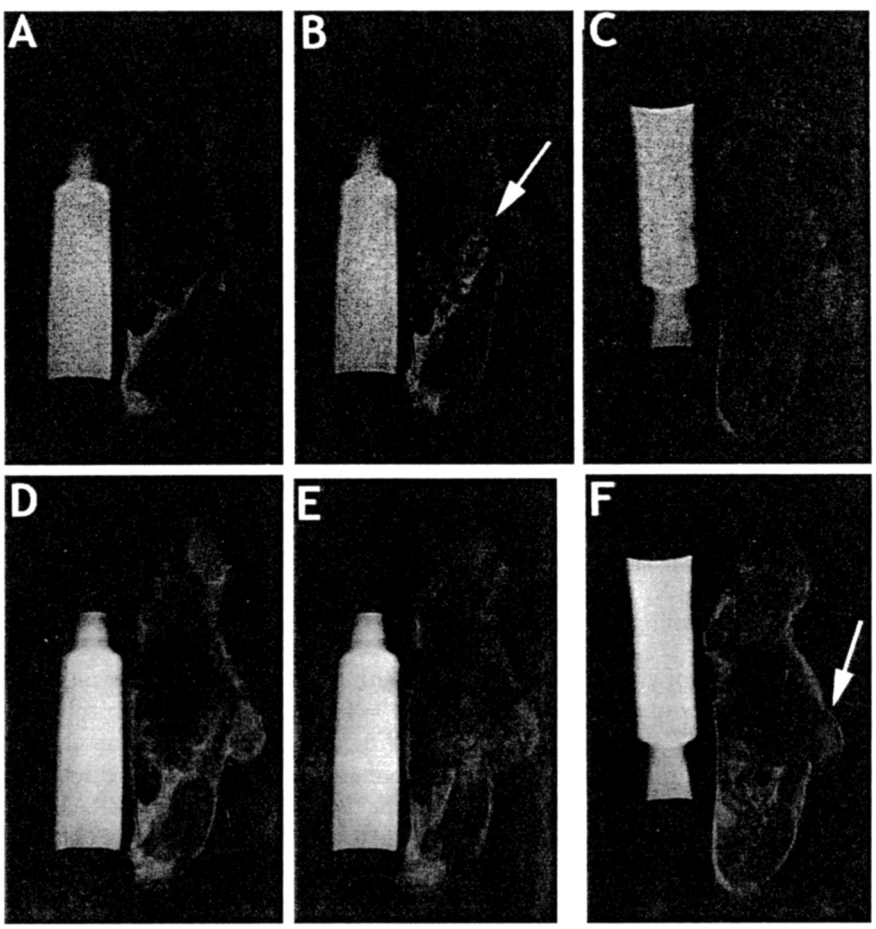

Fig. 3. Nude mouse human ovarian tumor xenografts expressing the hFR treated with folate-conjugated dendrimer. The enhanced kidney in T_1-weighted images (A, pre-injection; B, post-injection; C, 24 h post-injection) were used as an indication of contrast agent entry into circulation. The T_2-weighted images (D, pre-injection; E, post-injection; F, 24 h post-injection) show a significant enhancement of all tumors, $n = 5$, at the time point presented in 3F compared with those treated with Gd-HP-DO3A at the same time point ($P = 0.025$). A 1-mM vial of Gd-HP-DO3A was placed underneath the mouse.

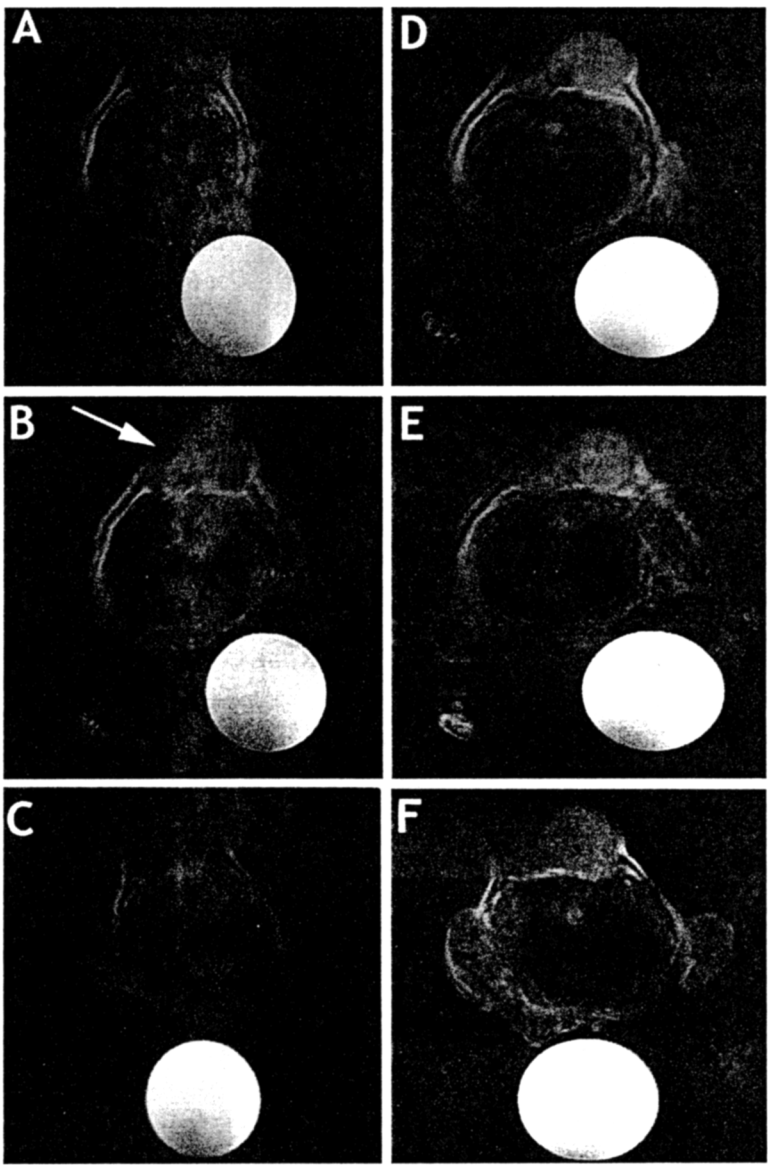

Fig. 4. Nude mouse human ovarian tumor xenografts expressing the hFR treated with Gd-HP-DO3A. The T_1-weighted images (A, pre-injection; B, post-injection; C, 24 h post-injection) show a heterogeneous distribution after injection that is not present 24 h later. The T_2-weighted images (D, pre-injection; E, post-injection; F, 24 h post-injection) do not show a change in contrast enhancement 24 h post-injection, 4F. A 1-mM vial of Gd-HP-DO3A was placed underneath the mouse.

signal intensity 24 h after injection of the folate-conjugated dendrimer. These data are significantly different ($P = 0.024$) from those obtained with the hFR-positive tumor xenografts, OVCA 432 cells, following 24 h after the injection (Table 1).

Next, we wanted to show whether the 0.06 mmol Gd kg^{-1} folate–dendrimer can be competed off with 0.3 mmol kg^{-1} of free folic acid, a $\sim$20–40-fold molar excess with respect to folate. A simultaneous injection of the free folic acid and the folate–dendrimer ($n = 4$) showed that under T_2-weighted conditions, 24 h following the injection, there was no decrease in PCE (Table 1). Results also show that the 24 h decrease observed with the folate–dendrimer alone was significantly lower, $P = 0.041$, compared with the folate competition study. We also wanted to know how the percent contrast enhancement of the competition compared with those of the saline-treated animals. As expected, following 24 h there is no difference in PCE, $P = 0.14$, between these two conditions, Table 1. In addition, the percent contrast enhancement of the folate competition after and 24 h after the injection were not significantly different, $P = 0.21$. This was also the case with the saline-treated animals, $P = 0.34$. The competition experiment provided additional evidence that the folate–dendrimer accumulation is mediated via a receptor saturable by folic acid.

4. Discussion

Currently, there is a need for contrast agents with specific localization within the targeted tissue of interest in order to improve lesion to normal tissue contrast, facilitating lesion diagnosis and disease prognosis. The aim of this study is to show specific targeting with MRI of the folate–dendrimer to ovarian tumor xenografts expressing the high affinity folate receptor. We first showed that the ^{153}Gd–folate–dendrimer is able to bind to folate-receptor-positive cells resulting in over a 2700% increase in binding compared with untreated cells. This accumulation was mediated by the presence of the folate receptor since only minor levels of binding were observed with folate-receptor-negative cells. In addition, the in vitro binding could be inhibited to the same levels as the folate-receptor-negative cells following free folic acid administration. The latter two controls demonstrate the specific interaction between the hFR and the folate–dendrimer.

Previously, we showed that the folate–dendrimer has over 8 times the transverse relaxivity (r_2) compared with a non-specific, extracellular fluid space agent at 4.7T [21]. Agents that accumulate in the tissue of interest and that have high transverse relaxivities, r_2, will decrease the relative signal intensity in T_2-weighted images of the tissue post-injection. Thus, even though the tissue contrast increases, the measured parameter described by the PCE will decrease. The larger the absolute value of the decrease, the greater the increase in tissue contrast. The PCE was quantitated to be -33% following 24 h of the folate–dendrimer administration. This decrease was not evident in tumors administered with the non-specific agent at the same time point [21].

Table 1
Percent contrast enhancement (PCE) under T_2-weighted conditions in hFR-positive or hFR-negative xenografts injected with the appropriate agent

Contrast agent	Post-PCE (%)	Post-24 h PCE (%)
Folate–dendrimer	-2.6 ± 14.0	$-33.1 \pm 52.0^{a,b,c,d}$
Gd-HP-DO3A	-1.1 ± 6.0^{a}	$+8.3 \pm 18.6^{a}$
Saline	-0.8 ± 6.1^{b}	$-7.5 \pm 21.2^{b,e}$
HFR-negative tumor	$+5.8 \pm 5.7$	$+5.9 \pm 16.3^{c}$
Folate competition	-0.4 ± 1.6	$+6.0 \pm 7.7^{d,e}$

[a] PCE 24 h of the folate–dendrimer is significant compared with Gd-HP-DO3A ($P = 0.025$) and the magnitude of post-PCE for Gd-HP-DO3A is significantly less than that of the folate–dendrimer ($P = 0.025$).

[b] The folate–dendrimer is significantly different from saline injection results at 24 h ($P = 0.047$) and post-injection ($P = 0.011$).

[c] The hFR-negative tumors are significantly different from the hFR positive tumors ($P = 0.024$).

[d] The folate–dendrimer is significantly different from the folate competition results at 24 h ($P = 0.041$).

[e] There is no difference between the folate competition and saline at 24 h ($P = 0.14$).

These results show that the folate-conjugated dendrimers are able to accumulate in ovarian tumors expressing the hFR, however, they do not elucidate the mechanism of the enhancement. Previously, we proposed that the accumulation could be due to a simple blood pool effect based on the longer plasma half-life of the dendrimer compared with the low molecular weight agent. It may also be due to a passive targeting of the folate–dendrimer into the tumor resulting from the leakage of the agent into the tumor interstitium via hyperpermeable capillaries often present in tumors [37]. These mechanisms, if occurring, would have been present in the folate-competition experiment as well as the receptor-negative tumor (Table 1). The lack of significant enhancement following 24 h in both of these experimental conditions provides evidence for the specific interaction of the folate–dendrimer by the hFR. These results, however, do not differentiate between the binding of the dendrimer to the hFR on the cell surface, in the tumor interstitium, or both. It is possible that the enhancement may result from a combination of a prolonged interstitial residence time and specific targeting. The hFR is bound to the extracellular surface of the plasma membrane by a glycosyl-phosphatidylinositol anchor [38] and is cleaved by phospholipase C [39]. This results in high concentrations of the soluble form of the receptor in the tumor interstitium [40,41]. The interstitial residence time of the targeted agent may increase with its specific binding to the soluble form of the receptor. Ideally, the results may also occur from the specific binding of the agent to the cell surface receptor, coupled with intracellular accumulation caused by receptor recycling [20] without soluble receptor binding. Finally, a combination of binding to the cell surface receptor and the soluble receptor may also occur. Regardless, the targeting is specific to the hFR and detectable by MRI.

The overexpression of the hFR is evident in ovarian cancer [28,42], however, its role in prognosis is not well characterized. Recently, it has been shown that high levels of the hFR may be an indication of cisplatin chemotherapy failure in patients [43]. The mechanism of this increased drug resistance are not clear and is hypothesized to be due to increased uptake of folates that may increase DNA repair of platinum crosslink damage. Alternatively, the role of the hFR in signal transduction in addition to folate accumulation may enable the cells to progress through the cell cycle in a faster manner [42,44].

5. Conclusions

Tumor physiology suggests that to achieve sufficient changes in the MRI signal intensity, the target site must be saturated with agents delivering large numbers of

Gd^{3+} ions per receptor. More recent theoretical calculations along with experimental evidence suggests that there is no physical limitation to imaging the classical biochemical receptors using currently available compounds, especially agents based upon dendrimers containing multiple simple gadolinium chelates [45]. In this study, we have shown that as few as 40 gadolinium chelates conjugated to generation four PAMAM dendrimers and having a total relaxivity of 1646 mM^{-1} s^{-1} can show specific enhancement of the hFR in ovarian tumors at 4.7*T*. The high total relaxivities reduces the number of ions required for contrast enhancement. The folate–dendrimer agent should add to the growing field of target-specific MRI contrast agents.

Acknowledgements

Supported by grants from the National Institutes of Health PHS-1-R29-CA61918, PHS-5-P41-RR05964, IS10RR06243, Systems and Integrative Biology Training Grant NIH T32 GM07143 to S.D.K. and Radiation Oncology Training Grant NIH T32 CA09067 to M.A.

References

[1] Brooks SE. Preoperative evaluation of patients with suspected ovarian cancer. Gynecol Oncol 1994;55:S80–90.
[2] Low RN, Saleh F, Song SYT, et al. Treated ovarian cancer: comparison of MR imaging with serum CA-125 level and physical examination — a longitudinal study. Radiology 1999;211:519–28.
[3] Brasch RC. Rationale and applications for macromolecular Gd-based contrast agents. Magn Reson Med 1994;22:282–7.
[4] Lauffer RB. Paramagnetic metal complexes as water proton relaxation agents for NMR imaging: theory and design. Chem Rev 1987;87:901–27.
[5] Unger EC, Totty WG, Neufeld DM, et al. Magnetic resonance imaging using gadolinium labeled monoclonal antibody. Invest Radiol 1985;20:693–700.
[6] Gohr-Rosenthal S, Schmit-Willich H, Ebert W, et al. The demonstration of human tumors on nude mice using gadolinium-labeled monoclonal antibodies for magnetic resonance imaging. Invest Radiol 1993;28:789–95.
[7] Mendonca-Dias MH, Lauterbur PC. Ferromagnetic particles as contrast agents for magnetic resonance imaging of the liver and spleen. Magn Reson Med 1986;3:328–30.
[8] Renshaw PF, Owen CS, McLaughlin AC, et al. Ferromagnetic contrast agents: a new approach. Magn Reson Med 1986;3(2):217–25.
[9] Cerdan S, Lotscher HR, Kunnecke B, et al. Monoclonal antibody-coated magnetite particles as contrast agents in magnetic resonance imaging of tumors. Magn Reson Med 1989;12:151–63.
[10] Weissleder R, Lee AS, Fischman AJ, et al. Polyclonal human immunoglobulin G labeled with polymeric iron oxide: antibody MR imaging. Radiology 1991;181:245–9.
[11] Weissleder R, Lee AS, Khaw BA, et al. Antimyosin-labeled monocrystalline iron oxide allows detection of myocardial infarct: MR antibody imaging. Radiology 1992;182:381–5.
[12] Reimer P, Weissleder R, Shen T, et al. Pancreatic receptors: initial feasibility studies with a targeted contrast agent for MR imaging. Radiology 1994;193:527–31.
[13] Reimer P, Weissleder R, Lee AS, et al. Receptor imaging: application to MR imaging of liver cancer. Radiology 1990;177:729–34.
[14] Kresse M, Wagner S, Pfefferer D, et al. Targeting of ultrasmall superparamagnetic iron oxide (USPIO) particles to tumor cells in vivo by using transferrin receptor pathways. Magn Reson Med 1988;40:236–42.
[15] Sipkins DA, Cheresh DA, Kazemi MR, et al. Detection of tumor angiogenesis in vivo by $\alpha_v\beta_3$-targeted magnetic resonance imaging. Nature Med 1998;4:623–6.
[16] Sipkins DA, Gijbels K, Tropper FD, et al. ICAM-1 expression in autoimmune encephalitis visualized using magnetic resonance imaging. J Neuroimmunol 2000;104:1–9.
[17] Wiener EC, Brechbiel MW, Brothers H, et al. Dendrimer-based metal chelates: a new class of magnetic resonance imaging contrast agents. Magn Reson Med 1994;31:1–8.
[18] Roberts JC, Adams YE, Tomalia D, et al. Using starburst dendrimers as linker molecules to radiolabel antibodies. Bioconjugate Chem 1990;1(5):305–8.
[19] Yang W, Barth RF, Adams D, et al. Intratumoral delivery of boronated epidermal growth factor for neutron capture therapy of brain tumors. Cancer Res 1997;57:4333–9.
[20] Wiener EC, Konda S, Shadron A, et al. Targeting dendrimer-chelates to tumors and tumor cells expressing the high-affinity folate receptor. Invest Radiol 1997;32:748–54.
[21] Konda SD, Aref M, Brechbiel M, et al. The development of a tumor targeting magnetic resonance contrast agent using the high affinity folate receptor: work in progress. Invest Radiol 2000;35:50–7.
[22] Zuckier LS, Rodriguez LB, Scharff MD. Immunologic and pharmacologic concepts of monoclonal antibodies. Semin Nucl Med 1989;28:166–86.
[23] Leamon CP, Low PS. Delivery of macromolecules into living cells: a method that exploits folate receptor endocytosis. Proc Natl Acad Sci 1991;88:5572–6.
[24] Leamon CP, Low PS. Cytotoxicity of mormordin-folate conjugates in cultured human cells. J Biol Chem 1992;267:24966–71.
[25] Leamon CP, Pastan I, Low PS. Cytotoxicity of folate-*pseudomonas* exotoxin conjugates toward tumor cells. J Biol Chem 1993;268:24847–54.
[26] Ross JF, Chaudhuri PK, Ratnam M. Differential regulation of folate receptor isoforms in normal and malignant tissues in vivo and in established cell lines. Cancer 1994;73:2432–43.
[27] Weitman SD, Weinberg AG, Coney LR, et al. Cellular localization of the folate receptor: potential role in drug toxicity and folate homeostasis. Cancer Res 1992;52:6708–11.
[28] Campbell IG, Jones TA, Foulkes WD, et al. Folate-binding protein is a marker for ovarian cancer. Cancer Res 1991;51:5329–38.
[29] Miotti S, Canevari S, Menard S, et al. Characterization of human ovarian carcinoma-associated antigens by novel monoclonal antibodies with tumor-restricted specificity. Int J Cancer 1987;39:297–303.
[30] Veggian R, Fasolato S, Menard S, et al. Immunohistochemical reactivity of a monoclonal antibody prepared against human ovarian carcinoma on normal and pathological female genital tissues. Tumori 1989;75:510–3.
[31] Coney LR, Tomassetti A, Carayannopoulos L, et al. Cloning of a tumor-associated antigen: MOv18 and MOv19 antibodies recognize a folate-binding protein. Cancer Res 1991;51:6125–32.
[32] Weitman SD, Weinberg AG, Coney LR, et al. Cellular localization of the folate receptor: potential role in drug toxicity and folate homeostasis. Cancer Res 1992;52:6708–11.

[33] Garin-Chesa P, Campbell I, Saigo PE, et al. Trophoblast and ovarian cancer antigen LK26. Am J Pathol 1993;142:557–67.
[34] Weitman SD, Lark RH, Coney LR, et al. Distribution of the folate receptor GP38 in normal and malignant cell lines and tissues. Cancer Res 1992;52:3396–401.
[35] Weitman SD, Frazier KM, Kamen BA, et al. The folate receptor in central nervous system malignancies of childhood. J Neurooncol 1994;21:107–12.
[36] Gor'Kov PL, Harris AB, Lauterbur PC. Immobilization system for rat brain imaging. Proc ISMRM 1998;3:2054.
[37] Jain JK. Transport of molecules in the tumor interstitium: a review. Cancer Res 1987;47:3039–51.
[38] Rijnboutt S, Jansen G, Posthuma G, et al. Endocytosis of GPI-linked membrane folate-receptor-[alpha]. J Cell Biol 1996;132:35–47.
[39] Luhrs CA, Slomiany BL. A human membrane-associated folate binding protein is anchored by a glycosyl-phospatidylinositol tail. J Biol Chem 1989;264:21446–9.
[40] Kane MA, Elwood PC, Portilla RM, et al. The interrelationship of the soluble and membrane-associated folate-binding proteins in human KB cells. J Biol Chem 1986;261:15625–31.
[41] Antony AC. The biological chemistry of folate receptors. Blood 1992;79:2807–20.
[42] Toffolli G, Cernigo C, Russo A, et al. Over expression of folate binding protein in ovarian cancers. Int J Cancer 1997;74:193–8.
[43] Toffoli G, Russo A, Gallo A, et al. Expression of folate binding protein as a prognostic factor for response to platinum-containing chemotherapy and survival in human ovarian cancer. Int J Cancer 1998;79:121–6.
[44] Corona G, Giannini F, Fabris M, et al. Role of folate receptor and reduced folate carrier in the transport of 5-methyltetrahydrofolic acid in human ovarian carcinoma cells. Int J Cancer 1998;75:125–33.
[45] Nunn AD, Linder KE, Tweedle MF. Can receptors be imaged with MRI agents. Q J Nucl Med 1997;41:155–62.